Chapter 6
Application: Diffusion Fields Reconstruction Under Heat Equation Constraint

Reconstructing a diffusion field from spatiotemporal measurements is an important problem in engineering and physics with applications in temperature flow, pollution dispersion, and disease epidemic dynamics. In such applications, sensor networks are used as spatiotemporal sampling devices and a relatively large number of spatiotemporal measurements may be required for accurate source field reconstruction. Consequently, due to limitations on the number of nodes in the sensor networks as well as hardware limitations of each sensor, situations may arise where the available spatiotemporal sampling density does not allow for recovery of field details. In this chapter, the above limitation is resolved by means of using the proposed algorithm. We propose to exploit the intrinsic property of diffusive fields as side information to improve the reconstruction results of classic CS.

6.1 Introduction

Many natural phenomenon in physics are governed by diffusion equation, including temperature flow, pollution dispersion, and disease epidemic dynamics. In such applications, sensor networks are used as spatiotemporal sampling devices to sample and reconstruct diffusion fields [1]. In contrast to general multidimensional signals, the effect of temporal and spatial down-sampling are not homogeneous. Generally, it is more expensive to increase the spatial sampling density as more sensors are needed in the network, while temporal sampling density is only limited by each sensor hardware [2]. An efficient sampling scheme will have an impact on real world applications such as pollution detection [3] and plume source detection [4].

Inverse problems of the diffusive fields are generally ill-posed and require a relatively large number of measurements. Typically, such dense data sets are required to allow for accurate reconstruction of fine field details. In such cases, improving the acquisition requirements of the hardware in use through reducing the sampling density would unavoidably produce aliasing artifacts. To overcome this limitation,

M. Rostami, *Compressed Sensing with Side Information on the Feasible Region*, SpringerBriefs in Electrical and Computer Engineering,
DOI: 10.1007/978-3-319-00366-5_6, © The Author(s) 2013

we apply the proposed algorithm for accurate reconstruction of sources from sub-Nyquist sampling rates.

In the current note, we consider spatiotemporal sampling and reconstruction of a 1-D diffusive field $u(x,t)$ governed by the heat equation:

$$\begin{aligned} \frac{\partial u(x,t)}{\partial t} &= \gamma \frac{\partial^2 u(x,t)}{\partial x^2}, \quad t \geq 0, \\ u(x,0) &= f(x) \end{aligned} \tag{6.1}$$

where γ is the diffusion coefficient, x denotes spatial domain variable, t denotes time domain variable, and $f(x)$ represents the initial field value.

If the initial field value is available, we can solve (6.1) for $u(x,t)$. However, in many situations, initial field value is not available [2], and it is not possible to derive $u(x,t)$ based on solely the partial differential equation constraint, as $u(x,t)$ varies dramatically with different initial condition. In these situations, we can measure spatiotemporal samples and use them to reconstruct $u(x,t)$.

Here, we take advantage of CS for efficient field sampling. It seems to be natural to reconstruct the source field using the fact that it satisfies the partial differential equation in (6.1) more efficiently. Specifically, we propose new CS formulation that incorporates the side information derived from (6.1) to improve the reconstruction quality of the standard CS, while resulting in substantial reduction in the required sampling density. We show that our efficient CS formulation can reduce the dimension of the feasible region in field reconstruction, resulting in better reconstruction quality.

6.2 Diffusive Compressive Sensing

Let $u(x,t)$ represents an original diffusive field which satisfies (6.1). For the sake of convenience, $u(x,t)$ is assumed to be defined over a finite-dimensional, uniform, rectangular lattice in $\mathbb{R}^2$. The discretized version of this field can be represented in a matrix $X \in \mathbb{R}^{N \times M}$. We assume that this field is sampled via a sensor network with N_s nodes which are deployed uniformly in the space and each sensor collects N_t uniform samples in time. Clearly, we have $m = N_t N_s$ measurements which can be represented in a matrix $Y \in \mathbb{R}^{N_s \times N_t}$ with $m = N_s N_t \leq NM = n$. X and Y can be concatenated into two column vectors $\mathbf{x}$ and $\mathbf{y}$ by means of lexicographic ordering, respectively. It is assumed that the observed version $\mathbf{y}$ of the vector $\mathbf{x}$ is obtained as $\mathbf{y} = \Psi \mathbf{x}$, where Ψ is a subsampling matrix which accounts for the effect of uniform downsampling. It is also assumed that $\mathbf{x}$ admits sparse representations with respect to a linear transformation W, $\mathbf{x} = W\mathbf{c}$. Finally, in order to apply CS to the problem, it is assumed that null(Φ) satisfies SSP by choosing Ψ and W properly.

Under the above conditions, CS-based reconstruction of the representation coefficients $\mathbf{c}$ can be performed according to (1.3). Our proposed diffusive CS algorithm uses the fact that $u(\cdot,\cdot)$ satisfies (6.1). Let D_x and D_t denote the matrices of dis-

crete partial differences in the spatial and time directions, respectively. Then, the discretized version of the constraint (6.1) suggests that

$$D_t \mathbf{x} = \gamma D_x D_x \mathbf{x} \rightarrow (D_t - \gamma D_x D_x) W \mathbf{c} = 0. \tag{6.2}$$

Let $B := (D_t - \gamma D_x D_x) W$, $\Phi' = \begin{bmatrix} \Phi \\ B \end{bmatrix}$, $\mathbf{y}' = \begin{bmatrix} \mathbf{y} \\ 0 \end{bmatrix}$, and $\mathbf{n}' = \begin{bmatrix} \mathbf{n} \\ 0 \end{bmatrix}$, then:

$$\mathbf{y}' = \Phi' \mathbf{c} + \mathbf{n}'. \tag{6.3}$$

Algorithm 1: Diffusive Compressive Sampling

1. *Data:* $\mathbf{y}$, δ, γ and $\lambda > 0$
2. *Initialization:* For a given transform matrix W and matrices/operators Ψ, D_x, D_t, preset the procedures of multiplication by $A = \Psi W$, A^T, B and B^T.
3. *Diffusive field recovery:* Starting with an arbitrary $\mathbf{c}^{(0)}$ and $p^{(0)} = 0$, iterate (4.28) until convergence to result in an optimal $\mathbf{c}^*$.
   a. Use CS solver algorithm of [5] for solving the optimization problem in (4.28).
   b. Update the vector of Bregman variables $p^{(t)}$.
4. *Source recovery:* Use the estimated (full) sparse representation $\mathbf{c}^*$ to recover the values of $\mathbf{x} = W\mathbf{c}^*$.

Note that the problem (6.3) is an instance of the problem (3.3) and can be studied in the proposed CS framework. Algorithm 1 summarizes all the diffusive CS algorithmic steps.

6.3 Experimental Results

The proposed algorithm is tested over three different solutions of the heat equation (6.1) as the source field, denoted by $u_1(\cdot,\cdot)$, $u_2(\cdot,\cdot)$, and $u_3(\cdot,\cdot)$ for different boundary and initial conditions. The fields are assumed to be defined over the lattice $[0, 2\pi] \times [0, 1] \subset \mathbb{R}^2$, uniformly discretized with $M = N = 128 \rightarrow n = 16,384$. We set the boundary conditions to be non-homogeneous for $u_1(\cdot,\cdot)$ and $u_2(\cdot,\cdot)$, and homogenous Neumann condition for $u_3(\cdot,\cdot)$. The initial conditions are chosen to be $f_1(x) = x$, $f_2(x) = \delta(x - \pi)$ (local point source), and $f_3(x) = \Pi(0, \pi)$ for each case, respectively. The subsampling matrix Ψ is assumed to downsample the source field uniformly with downsampling d_t and d_s factor in time and spatial domains, respectively:

Table 6.1 PSNR comparisons of diffusion field recovery results for noise level of 10 dB

d_s	1	2	2	1	4	4	1	8	8	1	16	16
d_t	2	1	2	4	1	4	8	1	8	16	1	16
PoS	50 %	50 %	25 %	25 %	25 %	6.25 %	12.5 %	12.5 %	1.56 %	6.25 %	6.25 %	0.39 %
PSNR comparison (in dB) for $u_1(\cdot,\cdot)$												
CS	14.07	20.04	13.57	6.73	7.41	5.72	0.65	0.62	−0.07	−0.51	−0.58	−0.06
DCS	24.95	25.22	21.61	21.46	21.43	14.96	17.36	17.88	11.61	14.00	14.50	10.45
PSNR comparison (in dB) for $u_2(\cdot,\cdot)$												
CS	14.03	19.97	13.70	12.38	15.54	11.57	6.79	7.20	5.87	0.61	0.58	−0.08
DCS	25.10	25.17	21.54	23.07	23.31	17.59	21.31	21.70	14.92	17.28	18.06	11.61
PSNR comparison (in dB) for $u_3(\cdot,\cdot)$												
CS	16.71	19.63	14.16	16.04	13.04	10.91	0.13	0.03	−0.37	−0.58	−0.59	−0.07
DCS	21.87	21.52	18.87	18.78	18.33	12.82	15.32	14.93	9.80	12.33	11.88	8.64

$$Y(i,j) = X(d_s i, d_t j), \quad 1 \le i \le N_s, 1 \le j \le N_t \tag{6.4}$$

For sparse representation basis, W was selected to be a four-level orthogonal wavelet transform using the nearly symmetric wavelets of Daubechies with five vanishing moments and $\delta = 0.5, \lambda = 0.001, \gamma = 1$.

For the purpose of comparison, we have compared our algorithm with classic CS approach in terms of reconstruction SNR. The results of this comparison are summarized in Tables 6.1 and 6.2 for different levels of noise and different percentage of the samples (PoS) in each table. In each table results for downsamling factors of 2, 4, 8, 16 in different directions are provided. As expected, for all cases one can see that DCS results in substantially high values of output SNR as compared to classic

Table 6.2 PSNR comparisons of diffusion field recovery results for noise level of 40 dB

d_s	1	2	2	1	4	4	1	8	8	1	16	16
d_t	2	1	2	4	1	4	8	1	8	16	1	16
PoS	50 %	50 %	25 %	25 %	25 %	6.25 %	12.5 %	12.5 %	1.56 %	6.25 %	6.25 %	0.39 %
PSNR comparison (in dB) for $u_1(\cdot,\cdot)$												
CS	14.95	23.45	14.19	6.88	7.56	6.01	0.70	0.61	−0.06	−0.51	−0.57	−0.06
DCS	25.22	25.28	21.66	21.27	21.54	14.97	17.41	17.96	11.63	14.00	14.53	10.49
PSNR comparison (in dB) for $u_2(\cdot,\cdot)$												
CS	14.60	23.48	14.13	6.91	7.57	6.01	−0.08	−0.51	−0.57	−0.43	−0.58	−0.06
DCS	25.21	25.28	21.60	21.27	21.55	14.98	13.96	11.61	10.53	9.44	10.35	6.14
PSNR comparison (in dB) for $u_3(\cdot,\cdot)$												
CS	17.41	20.33	14.46	16.05	13.20	10.91	−0.07	−0.07	−0.35	−0.60	−0.61	−0.07
DCS	21.92	21.53	18.79	18.78	18.23	12.87	15.41	15.01	9.83	12.30	11.87	8.50

CS, which implies a higher accuracy of field reconstruction. A close look on both tables reveals interesting results of the proposed algorithm. Note if we downsample a source field in one direction with the same downsampling factor, regardless of the direction, the resulting number of measurements are the same. Now consider those columns of tables with the same downsampling factor but different direction, e.g. first and second column, while for the case of classic CS the reconstruction quality differs in both tables, the quality of reconstruction for the case of DCS is similar. This can be explained through different correlations of the samples in different dimensions. From (6.2) one concludes that a field sample $X(i, j)$ is correlated with $X(i + 1, j)$ and $X(i + 2, j)$ in spatial domain while it is only correlated with $X(i, j + 1)$ in time domain. In other words dependency of the samples are not the same in time and spatial domain and it is harder to reconstruct the field when we lack time samples which is reflected in CS reconstruction results. In contrast, when we apply DCS these dependencies are considered as an additional data and thus the reconstruction quality is similar and is independent of downsampling direction. Generally, when we encounter insufficient spatial samples, oversampling in time domain is used to compensate [2]. Our result indicates that DCS can recover the source with less time samples which can be translated as energy saving in sensor nodes.

Another important result is on robustness of the proposed scheme towards insufficient samples. Consider a row in Tables 6.1 or 6.2, it can be seen that as the downsampling factor increases the reconstruction quality for classic CS degrades severely and for downsampling factors of 8 and 16 almost no information is recovered. While for the case of DCS, the algorithm is robust and even when we downsample a field with factor of 16 in both directions, using almost 0.4 % of the samples, it still can recover some information. For better comparison Fig. 6.1 depicts performances of CS and DCS algorithm for a range of downsampling factors with $d_t = 1$, $SNR = 40\,\text{dB}$, and $u_2(\cdot, \cdot)$. It can be seen that for the case of CS, the reconstruction quality degrades sharply for downsampling factors greater than 4 while diffusive CS is robust towards downsampling. This can be explained by the constraint exploited by DCS. The constraint $B\mathbf{c}' = 0$ in (4.27), can be considered as extra measurements of the sparse source which can compensate for insufficient real measurements. This can explain while the difference between CS and diffusive CS is negligible for small downsampling factors, why it becomes considerable as the scaling factor increases. When we have enough information to recover the source then constraint (6.2) does not provide considerable information but when we lack enough information, this constraint becomes more important.

A comparison between the result of Tables 6.1 and 6.2 also reveals that although reconstruction quality degrades as the additive noise power of measurements increases but DCS seems more robust towards the noise. To investigate the robustness of the proposed algorithms towards measurement noises, its performances has been compared for a range of SNR values (as a measure for noise power) with classic CS for the case $d_t = 2, d_s = 2$ and $u_3(\cdot, \cdot)$. The results of this comparison are summarized in Fig. 6.2. As expected in both cases the reconstruction quality degrades by decreasing SNR, but this dependency is more critical for classic CS, which results in steeper graph in Fig. 6.2. Again, this can be explained by the constraint exploited by DCS

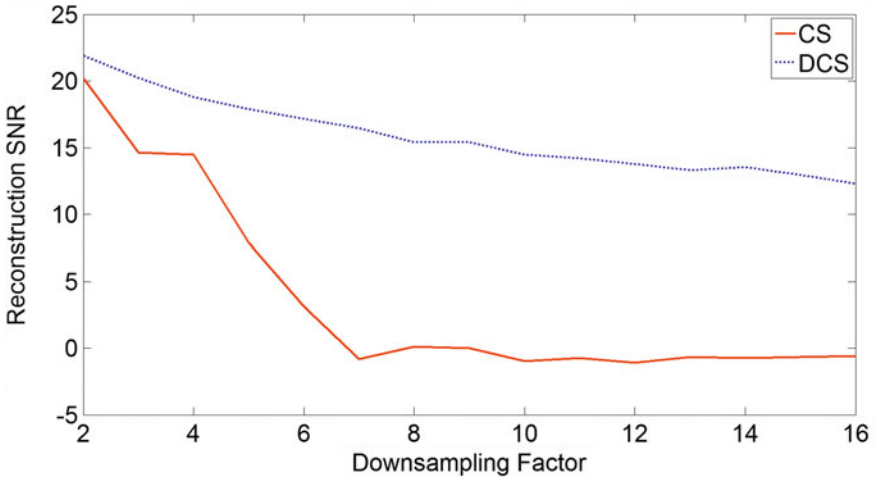

Fig. 6.1 SNR of field reconstruction as a function of spatial downsampling factor. Here, the *solid* and *dashed lines* correspond to classic CS and DCS, respectively, and $d_t = 1$

which restricts the feasibility region for an optimal solution. Moreover, as explained the constraint $B\mathbf{c}' = 0$ in(4.27), can be considered as extra measurements of the sparse source. These measurements are noise free and consequently one concludes that if we use this constraint, the reconstruction algorithm will become more robust towards the noise power. Intuitively one can say that since $\mathbf{n} \in \mathbb{R}^m$, $\mathbf{n}' \in \mathbb{R}^{n+m}$, and

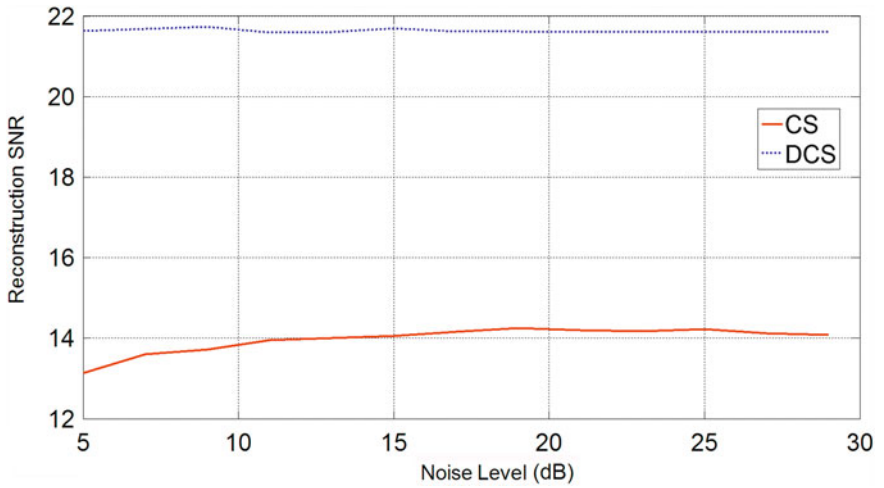

Fig. 6.2 SNR of field reconstruction as a function of noise SNR. Here, the *solid* and *dashed lines* correspond to classic CS and DCS, respectively, and $d_t = 2, d_s = 2$

$\|\mathbf{n}'\|_2 = \|\mathbf{n}\|_2$, the noise power has been multiplied by $\frac{m}{n+m} < 1$. This fact represents another advantage of incorporating the diffusive field constraints in the process of field recovery.

6.4 Summary

In this chapter, the problem of diffusive field reconstruction using sub-Nyquist sampling rates is studied. An efficient CS-based approach has been proposed to simplify the measuring devices and improve the device resolution. The proposed method applies CS for field reconstruction subject to an additional constraint, which stems from the intrinsic property of a diffusive field. Experiments confirm the source estimates by diffusive CS have better quality as compared to the case of classic CS and comparable as to the case of dense sampling. One direction for future work is applying the algorithm in designing the sampling devices for diffusive field reconstruction. Applying the algorithm in the sampling device structure will improve the capability of reconstructing diffusive field details in the presence of low density measurements. Another direction is to understand the performance under partial model knowledge.

References

1. P.C. Hansen, Rank-Deficient and Discrete Ill-Posed Problems: Numerical Aspects of Linear Inversion, vol. 4 (Society for Industrial Mathematics, 1987)
2. J. Ranieri, A. Chebira, Y.M. Lu, M. Vetterli, Sampling and reconstructing diffusion fields with localized sources, in *Proceedings of IEEE International Conference on Acoustics, Speech and Signal Processing* (IEEE, Prague, Czech, May 2011), pp. 4016–4019
3. A. El Badia, T. Ha-Duong, An inverse problem in heat equation and application to pollution problem. Inverse Ill Posed Probl. **10**(6), 585–600 (2002)
4. D.M. Moreira, T. Tirabassi, J.C. Carvalho, Plume dispersion simulation in low wind conditions in stable and convective boundary layers. Atmos. Environ. **39**(20), 3643–3650 (2005)
5. W. Yin, S. Osher, D. Goldfarb, J. Darbon, Bregman iterative algorithms for ℓ_1-minimization with applications to compressed sensing. SIAM J. Imaging Sci. **1**(1), 143–168 (2008)